Biomedical Optics EXPRESS

Holographic coherent anti-Stokes Raman scattering bio-imaging

Kebin Shi,[1,2] Perry S. Edwards,[1] Jing Hu,[3] Qian Xu,[1] Yanming Wang,[3] Demetri Psaltis,[4] and Zhiwen Liu[1,*]

[1]*Department of Electrical Engineering, The Pennsylvania State University, University Park, PA 16802, USA*
[2]*State Key Laboratory for Mesoscopic Physics, School of Physics, Peking University, Beijing 100871, China*
[3]*Department of Biochemistry and Molecular Biology, The Pennsylvania State University, University Park, PA 16802, USA*
[4]*School of Engineering, Ecole Polytechnique Fédérale de Lausanne, Lausanne, Switzerland*
**zliu@psu.edu*

Abstract: CARS holography captures both the amplitude and the phase of a complex anti-Stokes field, and can perform three-dimensional imaging by digitally focusing onto different depths inside a specimen. The application of CARS holography for bio-imaging is demonstrated. It is shown that holographic CARS imaging of sub-cellular components in live HeLa cells can be achieved.

OCIS codes: (180.5655) Raman microscopy; (090.1995) Digital holography; (180.6900) Three-dimensional microscopy.

References and links

1. J. E. Ludman, H. J. Caulfield, and J. Riccobono, *Holography for the New Millennium* (Springer Verlag, 2002).
2. Y. Pu, M. Centurion, and D. Psaltis, "Harmonic holography: a new holographic principle," Appl. Opt. **47**(4), A103–A110 (2008).
3. C. L. Hsieh, R. Grange, Y. Pu, and D. Psaltis, "Three-dimensional harmonic holographic microcopy using nanoparticles as probes for cell imaging," Opt. Express **17**(4), 2880–2891 (2009).
4. E. Shaffer, C. Moratal, P. Magistretti, P. Marquet, and C. Depeursinge, "Label-free second-harmonic phase imaging of biological specimen by digital holographic microscopy," Opt. Lett. **35**(24), 4102–4104 (2010).
5. O. Masihzadeh, P. Schlup, and R. A. Bartels, "Label-free second harmonic generation holographic microscopy of biological specimens," Opt. Express **18**(10), 9840–9851 (2010).
6. K. B. Shi, H. F. Li, Q. Xu, D. Psaltis, and Z. W. Liu, "Coherent anti-Stokes Raman holography for chemically selective single-shot nonscanning 3D imaging," Phys. Rev. Lett. **104**(9), 093902 (2010).
7. Q. Xu, K. Shi, H. Li, K. Choi, R. Horisaki, D. Brady, D. Psaltis, and Z. Liu, "Inline holographic coherent anti-Stokes Raman microscopy," Opt. Express **18**(8), 8213–8219 (2010).
8. R. F. Begley, A. B. Harvey, and R. L. Byer, "Coherent anti-stokes raman-spectroscopy," Appl. Phys. Lett. **25**(7), 387–390 (1974).
9. A. Yariv, "Phase conjugate optics and real-time holography," IEEE J. Quantum Electron. **14**(9), 650–660 (1978).
10. Y. R. Shen, *The Principles of Nonlinear Optics* (Wiley-Interscience, New York, 1984).
11. G. W. Burr, "Volume holographic storage using the 90 geometry," Ph.D. dissertation (California Institute of Technology, 1996).
12. M. Born, E. Wolf, and A. B. Bhatia, *Principles of Optics: Electromagnetic Theory of Propagation, Interference and Diffraction of Light* (Cambridge University Press, 1999).
13. A. Zumbusch, G. R. Holtom, and X. S. Xie, "Three-dimensional vibrational imaging by coherent anti-stokes raman scattering," Phys. Rev. Lett. **82**(20), 4142–4145 (1999).
14. D. J. Brady, K. Choi, D. L. Marks, R. Horisaki, and S. Lim, "Compressive holography," Opt. Express **17**(15), 13040–13049 (2009).
15. J. X. Cheng, A. Volkmer, L. D. Book, and X. S. Xie, "Multiplex coherent anti-stokes raman scattering microspectroscopy and study of lipid vesicles," J. Phys. Chem. B **106**(34), 8493–8498 (2002).
16. C. Heinrich, A. Hofer, A. Ritsch, C. Ciardi, S. Bernet, and M. Ritsch-Marte, "Selective imaging of saturated and unsaturated lipids by wide-field CARS-microscopy," Opt. Express **16**(4), 2699–2708 (2008).

1. Introduction

Since its inception, holography has found numerous applications in a wide range of scientific fields [1]. Classically, a hologram captures the change of the amplitude and the phase of an

#168344 - $15.00 USD Received 15 May 2012; revised 25 Jun 2012; accepted 25 Jun 2012; published 27 Jun 2012

optical wave due to its interaction with a specimen (e.g., reflection, transmission, or scattering) with the complex linear susceptibility ($\chi^{(1)}$). Consequently, holographic imaging usually relies on the differences in $\chi^{(1)}$ to provide image contrast. The merging of nonlinear optics and holography has created new opportunities to exploit the nonlinear susceptibility as a contrast mechanism. For instance, second harmonic holography utilizes $\chi^{(2)}$ (second-order nonlinear susceptibility) to provide image contrast and can record the second harmonic field generated by nano-crystal markers [2,3] or the endogeneous second harmonic radiation [4,5]. We recently proposed and demonstrated coherent anti-Stokes Raman scattering (CARS) holography [6,7], a special case of four wave mixing (FWM) holography which utilizes $\chi^{(3)}$ (third-order nonlinear susceptibility) as a contrast mechanism. This allows us to probe low-energy material excitations such as molecular vibrations and utilize the spectral response as a molecular "fingerprint" to provide image contrast. In particular, CARS holography fuses the three-dimensional (3D) imaging capability of holography with the high-sensitivity (up to ~five orders of magnitude improvement over the spontaneous Raman scattering [8]) and chemical selectivity of CARS into a new label-free, non-scanning, 3D imaging modality. Here we explore CARS holography for imaging live biological cells. In the following, we first discuss CARS holography by establishing the analogy between the generation of an anti-Stokes field and the diffraction by a volume hologram. This is then followed by experimental demonstration of holographic CARS imaging of endocellular components of HeLa cells.

CARS holography captures a complex anti-Stokes field by interfering it with a frequency-matched reference wave. Interestingly, the physical process of CARS, or more generally, FWM is also analogous to holography [9]. In a typical CARS process, a pump beam with the frequency ω_p interferes with a Stokes beam with the frequency ω_s to record a moving grating, or hologram, in a specimen of interest. The moving grating can be stored in the form of a molecular vibration if the frequency difference $\omega_p - \omega_s$ matches a resonant vibrational frequency. A probe beam, which oftentimes is the pump itself, can then read out the molecular vibration hologram to produce an anti-Stokes Raman signal. To further carry out this analogy, let us compare the governing equations of CARS [10] and diffraction of a volume hologram [11]:

$$(\nabla^2 + \frac{\omega_{as}^2}{c^2} n^2) E_{as} = -\frac{4\pi\omega_{as}^2}{c^2} \chi^{(3)}(x, y, z)(E_p E_s^*) E_{pr} \tag{1}$$

$$(\nabla^2 + \frac{\omega^2}{c^2} \bar{n}^2) E_d = -2\frac{\omega^2}{c^2} \bar{n} \Delta n E_{inc} \tag{2}$$

For simplicity, a scalar formalism is used here, i.e., the fields involved are assumed to be linearly polarized along the same direction. To arrive at Eq. (1), un-depleted excitation and a homogeneous refractive index *n* are assumed. E_{as}, E_p, E_{pr} and E_s are the fields associated with the anti-Stokes, pump, probe, and Stokes beams, $\chi^{(3)}(x, y, z)$ is the relevant third-order nonlinear susceptibility distribution, ω_{as} is the angular frequency of the generated anti-Stokes signal, and *c* is the speed of light in vacuum. In deriving Eq. (2), the Born approximation is utilized [12]. We have also neglected the term involving the dot product between the gradient of the permittivity and the field. $\bar{n}$ represents the average refractive index, Δn is the refractive index modulation resulted from a recorded hologram, E_{inc} and E_d are the incident and the diffracted field respectively, and ω is the angular frequency. Evidently, the molecular vibration plays the role of a hologram. When the molecular vibration is "read out" by a probe beam, an anti-Stokes signal is generated in a way similar to a holographic reconstruction process. Just as in conventional holography the reconstructed signal wave (i.e., E_d) contains

#168344 - $15.00 USD Received 15 May 2012; revised 25 Jun 2012; accepted 25 Jun 2012; published 27 Jun 2012

the image information of Δn, the generated anti-Stokes field (E_{as}) carries the image information of $\chi^{(3)}$. By digitally recording both the amplitude and the phase of the anti-Stokes field holographically, it allows us to digitally focus onto different depths inside a specimen and thereby realize 3D CARS imaging without scanning. We note that this is different from the optically sectioned scanning CARS microscopy [13], which directly images the three-dimensional nonlinear source distribution. For sparse objects, 3D tomographic reconstruction can be accomplished from a single hologram by using the technique of compressive holography [7,14].

2. Experiments and results

The schematic diagram of our experimental system is shown in Fig. 1. A nanosecond laser (Continuum Surelite III, fundamental wavelength: 1064 nm, second harmonic wavelength: 532 nm, repetition rate: 10 Hz, pulse duration ~5 ns, injection seeded) together with a tunable type II optical parametric oscillator provide the pump (also used as the probe) and Stokes beams for the CARS signal generation as well as the reference beam for recording CARS holograms. The pump/probe and Stokes beams were focused by a pair of lenses respectively (focal lengths: 750 mm and 150 mm), and spatially overlapped at the sample plane at an angle of about 20 degrees. The generated CARS/FWM image was then magnified by an imaging system consisting of an objective (numerical aperture: 0.42, focal length: 10 mm) and a lens (focal length: 500mm) and filtered by a band-pass filter (Chroma D800/30). The reference beam was first coupled into a section of a single-mode fiber (length: ~1 meter) and hence spatially filtered. It was subsequently collimated and combined with the CARS/FWM signal by using a pellicle beam splitter (reflectivity and transmittance: 8% and 92%, respectively).

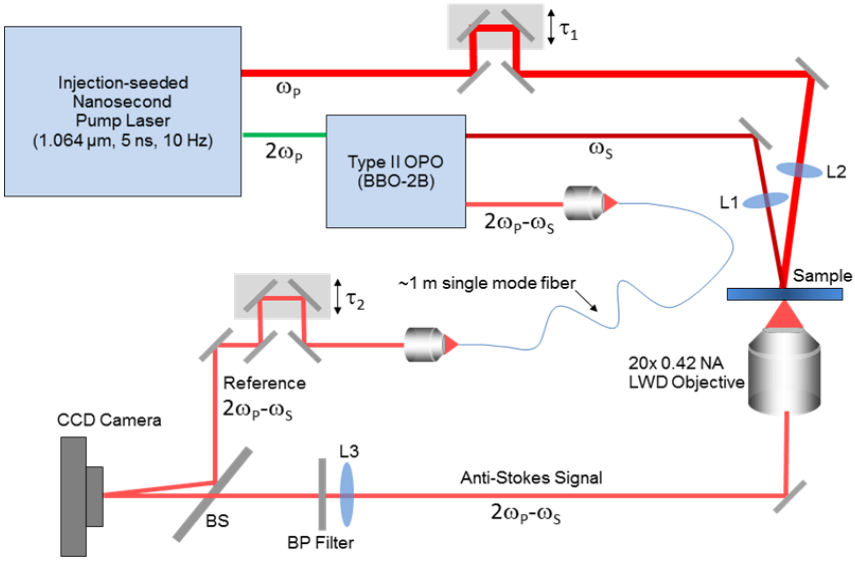

Fig. 1. Experimental setup of CARS holography. The fundamental beam with angular frequency of ω_p from the nanosecond laser was used as the pump and the probe for generating CARS or four wave mixing (FWM) signal. The frequency-doubled laser beam ($2\omega_p$) was used to pump the OPO to produce an idler beam at ω_s, which was utilized as the Stokes, and a signal beam at $2\omega_p - \omega_s$, which was used as the reference for recording CARS holograms. Note that the frequency of the reference beam automatically matches that of the CARS or FWM signal as the Stokes wavelength is tuned.

#168344 - $15.00 USD Received 15 May 2012; revised 25 Jun 2012; accepted 25 Jun 2012; published 27 Jun 2012

The two beams had a small angle (~2 degrees) between them. Their interferogram, or the resulting CARS/FWM hologram, was detected with a charge coupled device camera (Apogee 32ME).

The CARS holographic imaging system was utilized to image live cervical cancer HeLa cells, which were grown on glass coverslips in DMEM (Dulbecco's Modified Eagle Medium) supplemented with 10% fetal bovine serum and 1% penicillin-Streptomycin in a 5% CO_2 incubator at 37°C. The Stokes wavelength was tuned to excite the CH aliphatic vibrational mode at 2913cm^{-1}, which was reported to be rich in mitochondria clusters or lipid vesicles in Ref. [13,15]. To verify the CARS resonance, we detuned the wavelength of the Stokes beam from the resonant wavelength to record a sequence of wide-field CARS images as shown in Fig. 2. Figure 2(b) shows the CARS image when the frequency of the Stokes beam was tuned so that the 2913 cm^{-1} Raman vibrational mode can be resonantly excited. Figures 2(a) and 2(c) show the images acquired when the Stokes wavelength was detuned with Raman shifts of 2905 cm^{-1} and 2921 cm^{-1} respectively. It should be noted that as the wavelength was tuned the power of the Stokes beam may also vary slightly. However, Fig. 2 clearly shows the trend that as the detuning increases the signal strength reduces accordingly, consistent with the existence of a resonant mode.

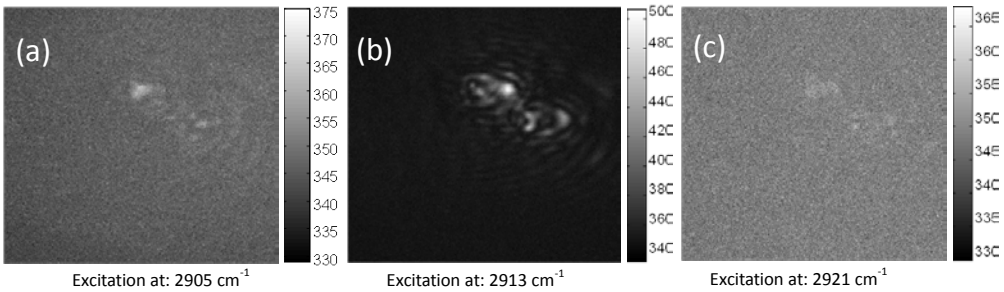

Fig. 2. Wide-field CARS images of HeLa cells around the resonant mode at 2913 cm^{-1} recorded by tuning the Stokes wavelength. CARS images (a) at 2905 cm^{-1}, (b) at 2913 cm^{-1}, (c) at 2921 cm^{-1}

We performed CARS holographic imaging of HeLa cells. The pulse energies of the pump and Stokes were adjusted to about 10 mJ and 4 mJ respectively. During the experiments, the cells were tested quickly after they were taken out of an incubator and kept alive during the measurements. Visual microscopic inspection followed to confirm that there was no apparent photo-damage to the cells during the experiment. However, sometimes samples were damaged due to defects or contaminants on the cover glass, which absorbed light and resulted in ablation. This problem may be alleviated by using picosecond laser systems, which can exhibit higher peak power with significantly less pulse energy. Figure 3(a) shows a CARS hologram of three HeLa cells (c.f., Fig. 3(d)) recorded with a single-shot exposure of a pair of pump and Stokes pulses (~5 ns), while Figs. 3(b) and 3(c) are the reconstructed field amplitude and phase distribution respectively. By performing digital back propagation, a sequence of images at different depth positions in the sample volume can be retrieved as shown in Figs. 3(e)-(h), where the sub-cellular components at different depth levels can be brought into focus sequentially.

To compare the digital focusing ability of CARS holography with analogue (manual) focusing in wide-field CARS microscopy [16], we captured a series of wide-field CARS images (i.e., direct images without the reference beam) of some HeLa cells by manually focusing onto different depth layers of the sample (i.e., through manual translation of the objective in the axial direction). Figures 4(a)-(e) show a series of holographically reconstructed CARS images of HeLa cells at different depth positions by using digital

#168344 - $15.00 USD Received 15 May 2012; revised 25 Jun 2012; accepted 25 Jun 2012; published 27 Jun 2012

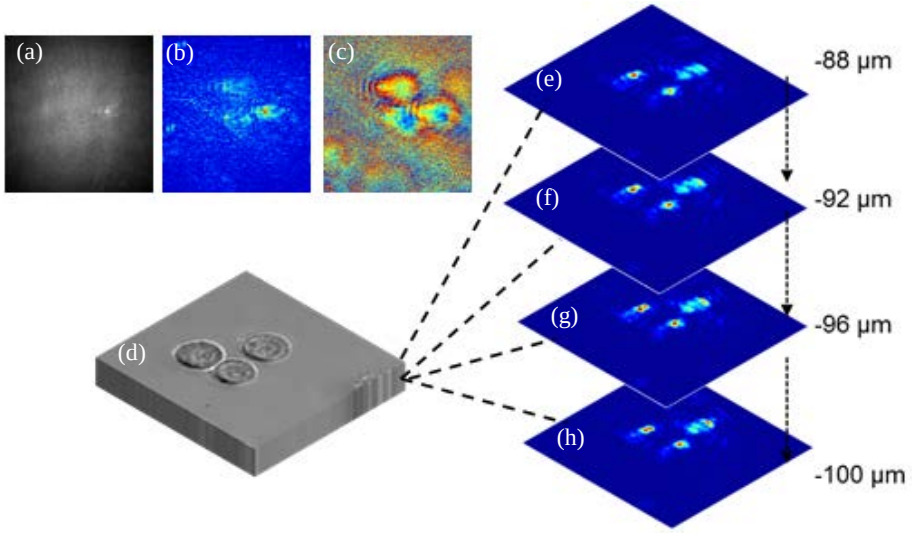

Fig. 3. 3D CARS holographic imaging of live HeLa cells. (a) Recorded CARS hologram. (b) Reconstructed field amplitude. (c) Reconstructed phase. (d) Micrograph of the three HeLa cells that were imaged. (e)-(h) Sequence of reconstructed CARS images at different depth positions in the sample volume, where the sub-cellular components at different depth levels can be brought into focus sequentially

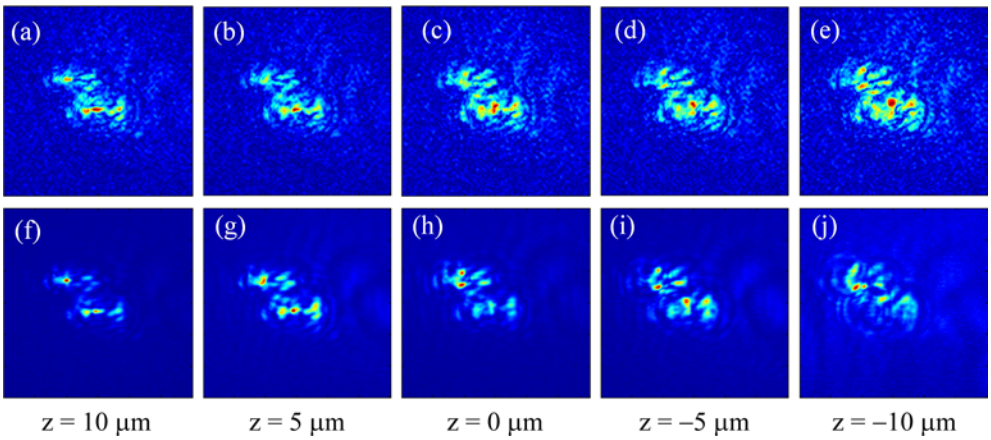

Fig. 4. Comparison of holographic CARS imaging (upper) and wide-field CARS imaging (bottom, with manual focusing) of HeLa cells at different depth positions (z: relative positions) demonstrating the equivalence of digital and analogue focusing. (a)-(e) Series of holographically reconstructed CARS images of HeLa cells at different depth positions by using digital propagation. (f)-(j) Corresponding manually focused wide-field CARS images. multiple-shot exposure was employed in the wide-field imaging scheme to increase the signal strength while single shot exposure was used in CARS holography.

propagation, while the corresponding manually focused wide-field CARS images are shown in Figs. 4(f)-(j). These two sets of images largely exhibit similar features although small differences exist partly due to the limited precision of the manual focusing. These results clearly demonstrate the equivalence of digital and analogue focusing. Note that multiple-shot exposure (~10 pulses) was employed in the wide-field imaging scheme to increase the signal strength. On the other hand, single shot exposure was used in CARS holography, which promises laser pulse duration limited speed but also results in relatively weak signal.

#168344 - $15.00 USD Received 15 May 2012; revised 25 Jun 2012; accepted 25 Jun 2012; published 27 Jun 2012

3. Summary

In summary, we have demonstrated non-scanning chemically selective 3D bio-imaging via holographic CARS microscopy. In addition to reconstructing the intensity distribution at different depth positions CARS holography also captures the phase information, which is not available in the wide-field imaging modality, and can lead to tomographic reconstruction through advanced digital processing algorithm (e.g., compressive holography [14]). Our imaging results on live HeLa cells indicate that CARS holography is useful as a practical tool for 3D cellular imaging. The unique ability of label-free and thus non-toxic imaging allows for long duration studies of sub-cellular components in live specimens. Furthermore, with the added capability of single-shot imaging, CARS holography has the potential to image fast biological processes at laser pulse duration limited speed.

Acknowledgments

K. Shi acknowledges the support from the National Science Foundation of China (NSFC# 11174019 and 11121091). Y. Wang acknowledges the support from the National Institute of Health (R01CA136856). D. Psaltis acknowledges the support from Nano-Tera (#530072 "NT-SSSTC-Optofluid"). Z. Liu acknowledges the support from the National Science Foundation (ECCS-0547475 and DBI-0649866).

#168344 - $15.00 USD Received 15 May 2012; revised 25 Jun 2012; accepted 25 Jun 2012; published 27 Jun 2012